The effect of heat treatment on pseudoelastic behavior of spark plasma sintered NiTi

Gülcan Özerim, Günay Anlaş, Ziad Moumni

Version of Record: https://www.sciencedirect.com/science/article/pii/S2352492822006766
Manuscript_f9546c6991ccba492dd7e41cffc904d6

The effect of heat treatment on pseudoelastic behavior of spark plasma sintered NiTi

Gülcan Özerim[a,b,*], Günay Anlaş[a], Ziad Moumni[b]

[a] Mechanical Engineering Department, Boğaziçi University, Istanbul, 34342, Turkey

[b] UME, ENSTA-Paris, Institut Polytechnique de Paris, 91120 Palaiseau, France

Abstract

Porous NiTi shape memory alloys are considered as artificial bio-materials for possible use in implant applications. Their extraordinary pseudoelastic response under uniaxial loading through phase change needs further analysis. The objective of this work is to show the effect of heat treatment on the pseudoelastic behavior of NiTi SMA produced by spark plasma sintering (SPS). NiTi samples were prepared from pre-alloyed Ti-50.7 at.% Ni powders of 100-150 µm average diameter, and subjected to a wide range of homogenization and/or aging at different temperatures and duration. Transformation characteristics of heat treated samples were obtained from DSC, their phase composition was identified using X-ray diffraction (XRD), and checked with scanning electron microscopy (SEM) and energy dispersive X-ray analysis (EDX). Instrumented micro-indentation was carried out to measure the hardness altered by aging. Uniaxial compression tests were performed on heat treated samples, and their pseudoelastic behavior was shown on the stress-strain diagrams; the results showed a variation in pseudoelasticity. In general, Ni concentration of the matrix resulted in partial-pseudoelastic behavior of samples. Homogenization prior to aging improved the pseudoelasticity of the SPSed NiTi. The pseudoelastic response of the samples that have not shown the expected full pseudoelastic behavior was enhanced by applying a considerably long period of homogenization and aging.

Keywords: NiTi; Porous; Heat treatment; Pseudoelasticity; Spark plasma sintering

1 Introduction

Porous NiTi shape memory alloys (SMAs) attracted interest in biomedical applications as a hard tissue replacement material with increased interfacial bonding, lower elastic modulus and density achieved with porosity [1–3]. In addition, the ability of NiTi to recover from large deformations through phase transformation (pseudoelastic behavior) increases its potential to be used as an implant material [2–4]. Porous NiTi parts can be produced starting from elemental or pre-alloyed Ni-Ti powders in different sizes and fractions [5, 6]. Spark plasma sintering (SPS) is one of the methods applied to metallic powders providing rapid fabrication compared to other sintering techniques such as conventional sintering (CS), hot isostatic pressing (HIP) or self-propagating high temperature synthesis (SHS) [1]. During the SPS process, powders are consolidated through simultaneous application of heat and pressure. Temperature is uniformly increased through pulsed DC current along with uniaxial pressure applied through graphite dies [7,8]. In the literature on SPS processed NiTi, most of the works focus on densification and microstructural (phase) evaluation [7,9–12] while achieving the pseudoelastic behavior after sintering is not straightforward. For the pseudoelastic response, NiTi must be loaded

*Corresponding author. E-mail address: gulcan.ozerim@boun.edu.tr

at a temperature around its critical austenite finish temperature (A_f), and its yield strength must be high to prevent plastic deformation [13]. Both criteria depend on the phase composition of the material. After sintering, NiTi compacts are cooled in a large temperature interval that results in uncontrolled formation of secondary phases such as Ti_2Ni, Ti_3Ni_4 or $TiNi_3$ among which the crucial contribution to the pseudoelastic behavior comes from precipitation of Ti_3Ni_4 [14, 15]. Homogeneous and coherent precipitation of Ti_3Ni_4, obtained mainly between $300 - 600°C$, increases the resistance against plastic deformation by the internal stress field generated around them [13, 15–19]. Therefore, NiTi samples need thermal treatment after spark plasma sintering to control the microstructure, hence the phase transformation and the mechanical behavior.

In the literature, many works focus on the effects of heat treatment of NiTi alloys produced by classical casting and then hot/cold working methods while studies on the heat treatment of SPS processed NiTi are limited. Zhao et al. [20] have produced NiTi samples using SPS starting from pre-alloyed Ti-50.9 at.% Ni powders; their dense and 13% porous samples showed a good pseudoelastic loop under uniaxial compression after a short time aging treatment (30 minutes at 320°C then water quenched). The same sintering and heat treatment processes were repeated by Nemat-Nasser et al. [21] who observed similar pseudoelastic behavior with 12% porous NiTi. Later, Butler et al. [22] have produced highly dense NiTi wires through spark plasma sintering and extrusion starting from fine elemental powders. Although their as-SPSed samples have shown transformation peaks in differential scanning calorimetry (DSC), they applied 15 minutes of aging at 500°C after sintering and extrusion which resulted in the expected pseudoelastic behavior under tension. Soba et al. [23] sintered elemental Ni-Ti powders by mixing them with TiO_2 powders to increase the strength of the alloy. Sintered compacts with 99.9% relative density were then hot extruded, solutionized at 1000°C, and aged at 500°C for an hour. The extruded and heat treated bars were then tested under uniaxial tension up to 3% maximum strain; although there were no clear stress plateau during unloading, 100% strain recovery was achieved. Lately, Salvetr et al. [24] studied the influence of heat treatment on the microstructure and the mechanical properties of a spark plasma sintered NiTi alloy, testing the specimens under high strain rate compression, and comparing their ultimate compressive strengths; but there was no discussion of the pseudoelastic behavior.

Previous works in the literature show that spark plasma sintered NiTi is expected to show a pseudoelastic loop similar to the one seen from bulk NiTi up to $12 - 13\%$ porosity [20–23]. With increasing porosity, however, the pseudoelastic response starts to differ and the recovery from deformation decreases [25–30]. Either highly dense or porous, SPSed NiTi is heat treated to enhance its pseudoelastic behavior, and there is a need to discuss the effect of heat treatment on the pseudoelastic behavior. The pseudoelastic behavior of NiTi alloys processed by hot isostatic pressing (HIP) and selective laser melting (SLM) has been studied by McNeese et al. [31] and Saedi et al. [32] respectively. But there is no work in the literature that studies the heat-treatment-pseudoelasticity relation of SPSed NiTi, especially the effect on the full recovery from strain.

The present work contributes to the literature by studying the effects of a wide range of heat treatment on the pseudoelastic behavior of a spark plasma sintered NiTi. The heat treated NiTi compacts were characterized in terms of shape memory characteristics and pseudoelasticity using calorimetric measurements, microstructural analyzes, and uniaxial compression tests. A detailed discussion was presented by comparing the effects of the heat treatments applied to the SPSed NiTi and the ones used in the literature.

2 Experimental procedure

Pre-alloyed Ti-50.7 at.% Ni powder of 100-150 µm nominal diameter, purchased from TLS Technik GmbH (Bitterfeld Germany), was consolidated using DR SINTER Fuji 515-S LAB Spark Plasma Sintering equipment. The powder was placed in a graphite die covered with graphite paper, and heated in a vacuumed chamber at 100°C/min rate, held at the target temperature for 5 minutes, and then cooled to room temperature. Average porosity, f_p, of the cylindrical compacts was calculated using $f_p = 1 - m/(\rho V)$ where m is the powder mass, $\rho_{NiTi} = 6.45$ g/cm^3 is the theoretical density of bulk NiTi, and V is the end volume of a cylinder. A porosity range up to 30% was achieved by changing the parameters. Details of the sintering parameters, resulting dimensions and porosity are presented in Appendix A (see Table A.1). Porosity can be decreased significantly by increasing the temperature or pressure as expected. However, when compared to the sintering parameters and resulting porosity (850°C, 50 MPa, 0% porosity) provided by Zhao et al. [20], remarkably higher temperature and pressure (1000°C, 60 MPa) were required with a comparable powder size to decrease the porosity. It is recognized that Zhao et al. [20] did not share any dimension which is known to affect the sintering parameters, resulting porosity and microstructure as studied by Olevsky et al. [33].

High density NiTi compacts were subjected to different combinations of homogenization and aging treatments to analyze the change in their pseudoelastic behavior. The target of homogenization is to dissolve the secondary phases or precipitates (e.g. Ti_2Ni, $TiNi_3$ and Ti_3Ni_4) that may form during sintering, thereby better controlling the aging process. Subsequent aging of NiTi alloys enhances the pseudoelastic behavior if coherent precipitation of Ti_3Ni_4 in small sizes is achieved [16, 19]. First, $20 - 60$ mg samples were cut from NiTi compacts for heat treatment and calorimetric tests. They were either first homogenized at 1000°C and then aged, or directly aged between $320 - 600$°C in an oven operated under air. The heat treatment categories that were used for the calorimetric analyzes are listed below:

- 1 h of direct aging in $320 - 500$°C temperature range.
- 2 h of homogenization and then 1 h of aging in $350 - 600$°C temperature range,
  2 h of homogenization and then aging from 30 minutes to 3.5 h at 500°C.
- 5 h of homogenization and then 24 h of aging at 350°C.

After either homogenization or aging, the samples were water quenched using tap water, and then mechanically polished with 500 grit silicon-carbide papers. Effect of heat treatment on transformation temperatures and paths were studied with a Setaram-131 differential scanning calorimeter at 10°C/min heating and cooling rate according to ASTM F2004-17 [34]. Phase composition of the samples were also analyzed in three categories. A Rigaku D/MAX-Ultima X-ray diffraction (XRD) equipment with a Cu-K_α anode was used around room temperature (20-25°C) in the range of 0° to 90° 2θ. The effect of aging time was shown by studying 1-5-18-24 h of aging after 5 h of homogenization.

Hardness measurements were carried out using a Ficherscope-HM2000 instrumented micro-indentation equipment with a diamond Vickers indentor. The sintered samples were cut into small sizes, hot mounted using an epoxy resin, and then mechanically polished starting with grit papers followed by diamond pastes until 1 µm final polish prior to testing. Indentation was performed at ambient temperature, around 27°C, where the samples were mostly in a mixed austenite - martensite or R-phase structure according to their DSC results. Load was increased from zero to 1000 mN in 20 s, and then decreased to zero at the same speed. The samples were indented at 10 random points; average Vickers hardness and percent of recovered energy were recorded.

Cylindrical compression test specimens were machined from the sintered compacts with an L/d ratio of two (5 mm diameter, 10 mm length). The specimens were subjected to three different heat

treatments to see the differences in their deformation under uniaxial compression: 1 h of direct aging; 2 h of homogenization and then 1 h of aging; 5 h of homogenization and then 24 h of aging, all samples being aged at 350°C. The samples were heated up to 100°C and then cooled down to the test temperature prior to uniaxial compression to increase the amount of austenite at the initial state. Compression tests were performed at 10^{-3} s^{-1} strain rate, until around 4% global strain, with a 30 kN Instron-5960 loading machine equipped with an environmental chamber controlling the temperature. Each sample was compressed twice: first at a temperature 5°C above A_f to observe the pseudoelastic behavior. Second test was performed at room temperature (27°C), that is below A_f, to observe the shape memory effect. The displacement data were directly obtained from the machine and the correction for the setup compliance was obtained experimentally as suggested by Instron.

3 Results and discussion

Figure 1 shows the DSC plot and the X-ray diffraction pattern of the powder. It is expected to be a mixture of the austenite-martensite phases around room temperature according to the DSC plot. The XRD pattern of the powder matched perfectly with the theoretical austenite and martensite peaks; there was no impurity in the starting material.

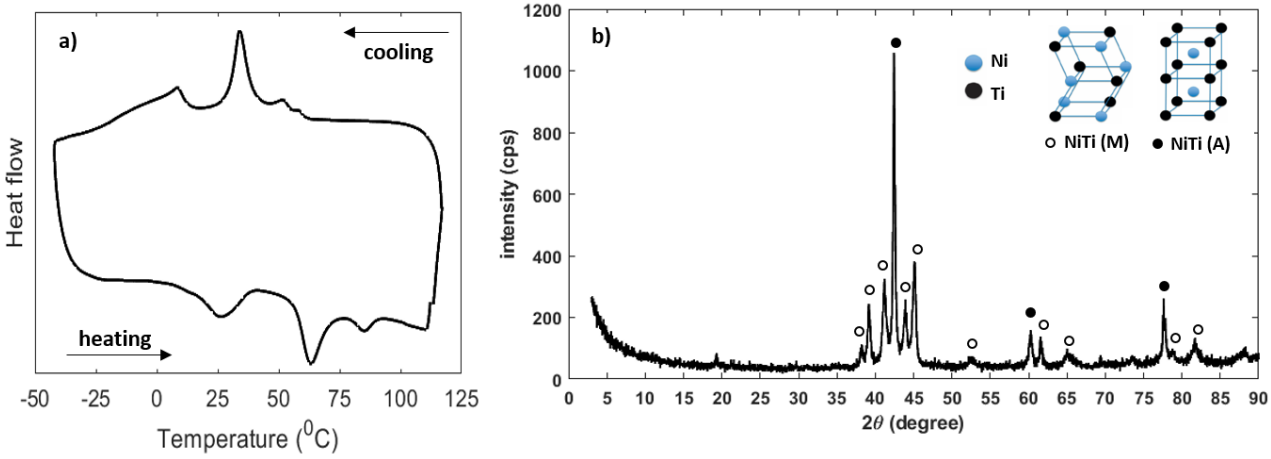

Figure 1: a) DSC plot, b) XRD pattern of the Ti-50.7 at.% Ni powder

Figure 2 shows the phase composition of the as-sintered sample by X-ray diffraction and scanning electron microscopy (SEM). Only the main peak area between 40-45 2θ was shown for a better focus. The XRD spectrum of the as-sintered sample revealed the presence of austenite and martensite phases together at room temperature. Twinned structure of martensite was visible in the SEM image in Figure 2b. Dark gray spots observed under SEM were matched with Ti_2Ni ($Ti_4Ni_2O_x$) phase as presented in the literature [5, 23, 31, 35, 36] which was also supported by the results of energy dispersive X-ray analysis (EDX). The composition of the matrix was found to be Ti-49.8 at.% Ni while composition of the dark gray spots was Ti-38at.%Ni which is very close to the theoretical atomic composition of Ti_2Ni. These regions were assumed to be Ni-rich solution of Ti_2Ni phase. Ti_2Ni was also detected by XRD with a low intensity as shown in Figure 2a, no Ti_3Ni_4 nor $TiNi_3$ phases were detected by XRD.

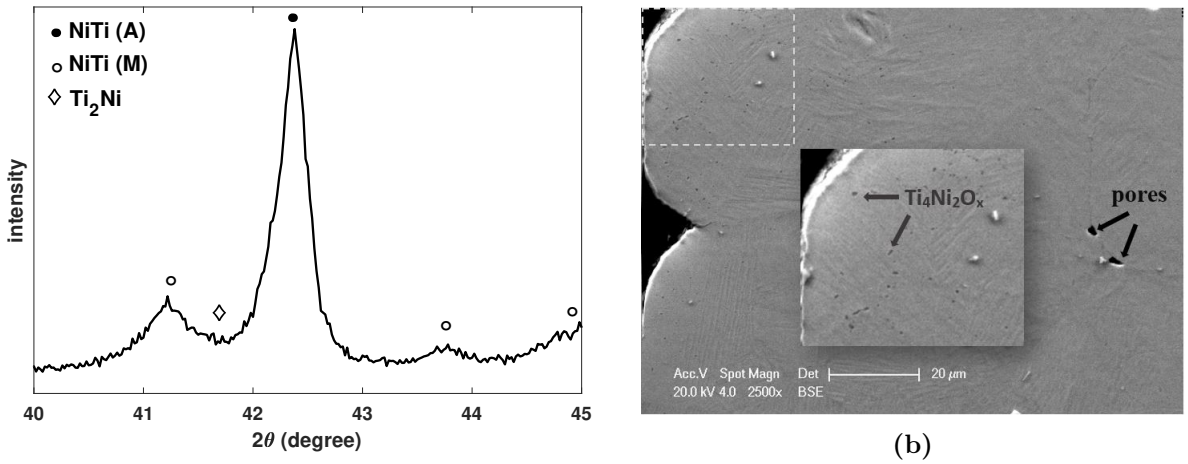

Figure 2: (a) X-ray diffraction pattern, (b) SEM image of as-sintered sample

Heat treatment may alter the transformation characteristics by changing the microstructure in Ni-rich NiTi alloys, therefore, NiTi samples are often heat treated to improve their pseudoelastic behavior. DSC plots can be used to observe the differences in their transformation sequence and temperatures. The DSC plots of the sintered and heat treated samples are shown in Figures 3, 4 and 5. The alloy that was not heat treated exhibited weak transformation peaks as shown in Figure 3; the austenite finish temperature was supposed to be higher than 80°C. The first sample tested was subjected to 30 min. of direct aging. Zhao et al. [20] and Nemat-Nasser et al. [21] observed the full pseudoelastic behavior from a similarly heat treated spark plasma sintered pre-alloyed Ti-50.9 at.% Ni powder under uniaxial compression. The material tested in this study did not show any clear transformation peak after the same treatment. Figure 3 shows the evolution in the DSC plots up to 1 h aging at different temperatures. The phase transformation peaks became visible at 1 h aging at 350°C. When the aging temperature was increased from 350°C to $400-500$°C, the phase transformation were more pronounced. The transformation curve is wavy and continues gradually in a large temperature interval when compared to the DSC plots of the samples that were first homogenized and then aged as presented in Figure 4. This type of multi-step transformation of NiTi was explained by inhomogenous distribution of Ti_3Ni_4 precipitates in the literature [16, 18].

DSC plots of the samples that were first homogenized for 2 h and then aged for an hour in 350-600°C temperature range are provided in Figure 4. After 2 h of homogenization, two distinct transformation peaks (one in the heating range, another one in the cooling range) were observed in the DSC plot which is typical for bulk NiTi alloys that are not subjected to aging treatment. Under certain temperature and duration, aging may promote R-phase transformation which manifests itself with a small temperature hysteresis between forward and reverse transformation peaks on a DSC plot [16, 19, 37]. DSC results obtained from the samples which were aged between $350-500$°C after 2 h of homogenization exhibited the characteristic transformation peaks between austenite and R-phases which was more clearly visible on the DSC plot of the sample corresponding to aging at 500°C. The R-phase formation through aging is expected until around 600°C according to the phase diagram of NiTi [15]. The DSC plot corresponding to 2 h of homogenization plus 1 h of aging at 600°C showed one-step transformation between austenite and martensite phases similar to the only homogenized one; the result is consistent with the literature [15, 19, 37]. 350°C, 400°C and 450°C aging temperatures did not show significant changes in the DSC plots. Their transformation peaks were found to be in the temperature range of $20-40$°C, and mainly one-step transformation between austenite and R-phases was observed. At 500°C aging temperature, a second transformation peak indicating the transformation from R-phase to martensite was detected near the lower temperature edge, however, the peak intensity is small to recognize in Figure 4.

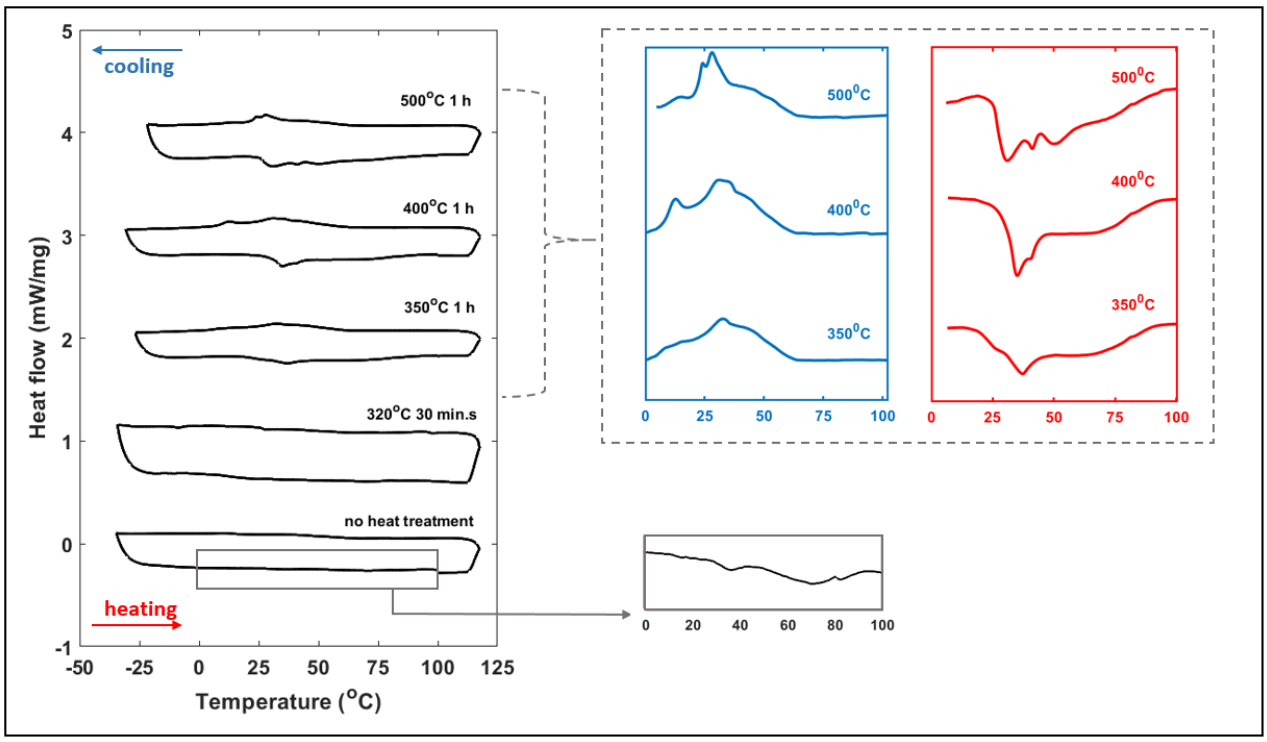

Figure 3: DSC plots of the samples subjected to direct aging treatment. (Curves of no heat-treated sample and the material after aging for 30 min. at 320°C are plotted for comparison)

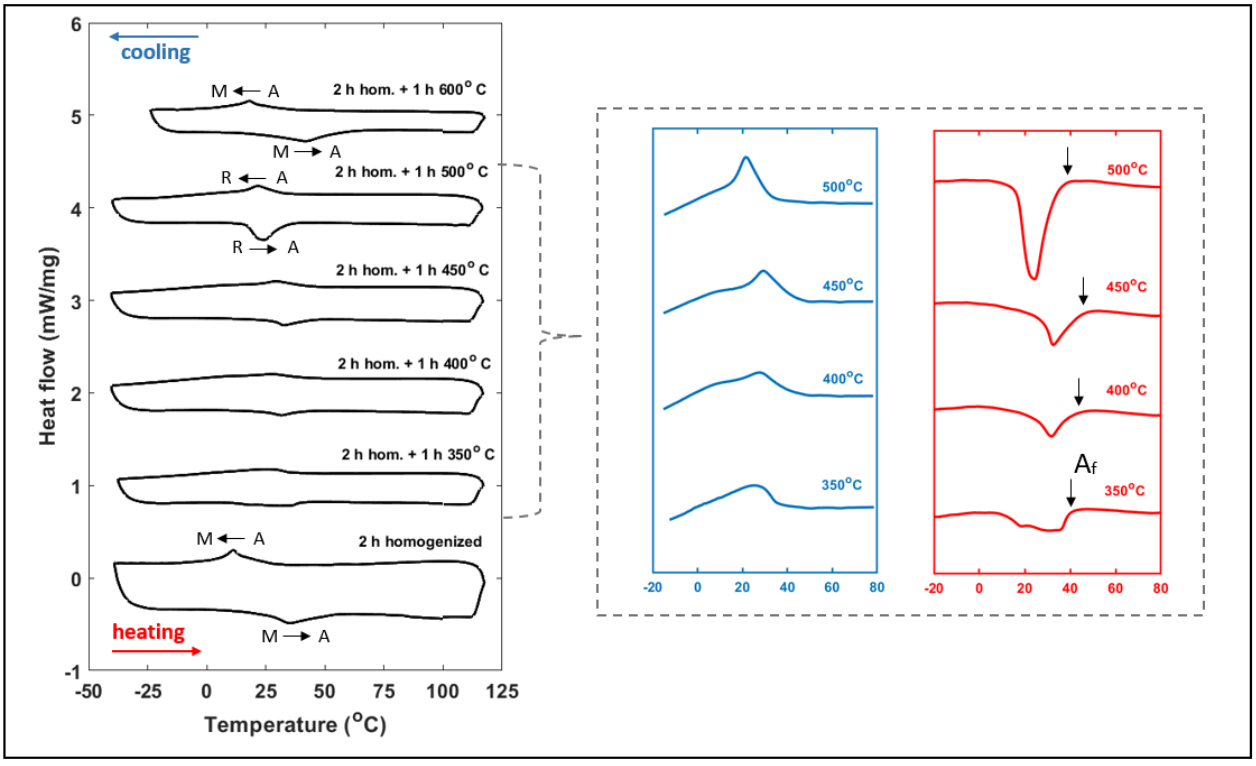

Figure 4: DSC plots of the samples subjected to 2 h of homogenization and then 1 h of aging treatment. The small vertical arrows indicate the austenite finish temperature (A_f).

Figure 5 shows evolution of the transformation peaks in time while keeping the aging temperature at 500°C. After 2 h of aging, the second transformation peak from R-phase to martensite became more pronounced. This two stage transformation behavior that was initially observed in cooling also appeared in heating by increasing the aging time to 3.5 h. In addition, the A_f temperature significantly increased by 3.5 h of aging (around 25 °C) at 500°C. This result was attributed to a possible decrease in the Ni concentration of the matrix due to growing size of Ti_3Ni_4 precipitates by increasing the aging time. The increase in the precipitate size when aging NiTi alloys at 500°C was reported by Gall et al. [17] and Aboutalebi et al. [37] earlier.

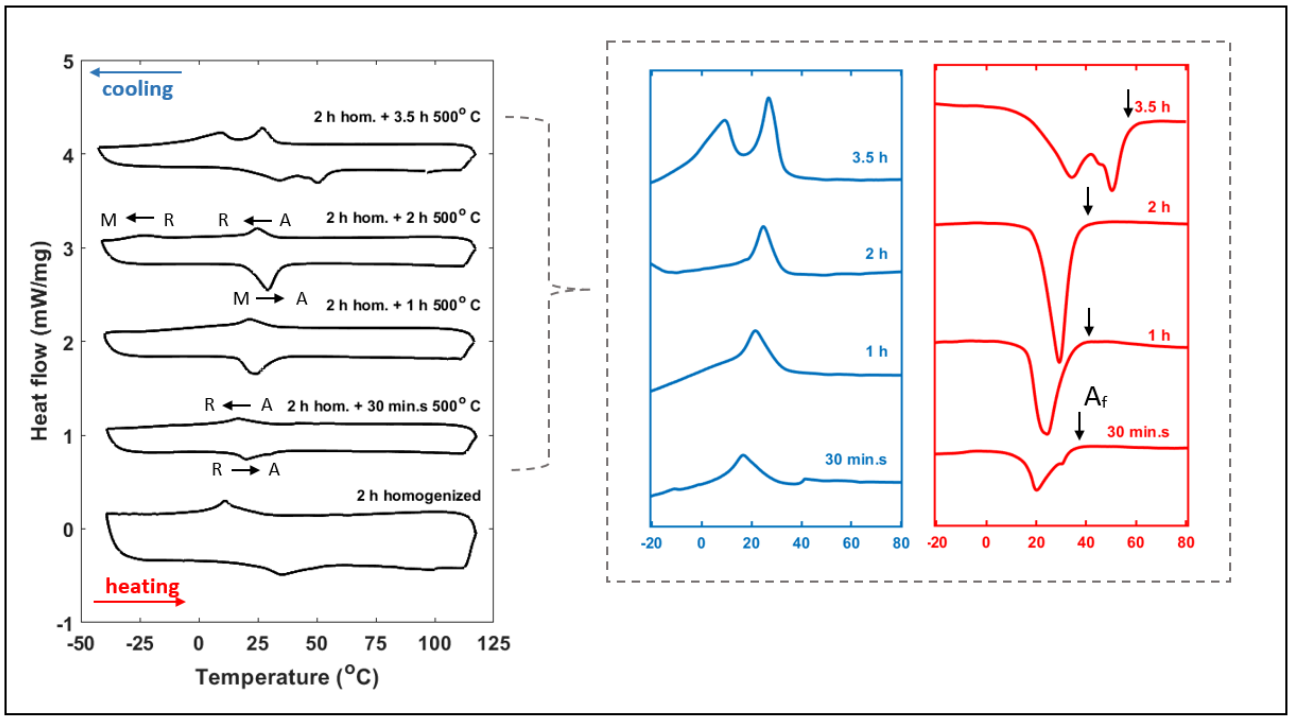

Figure 5: DSC plots of the samples subjected to 2 h of homogenization and then aging at 500°C by varying time. The small vertical arrows indicate the austenite finish temperature (A_f).

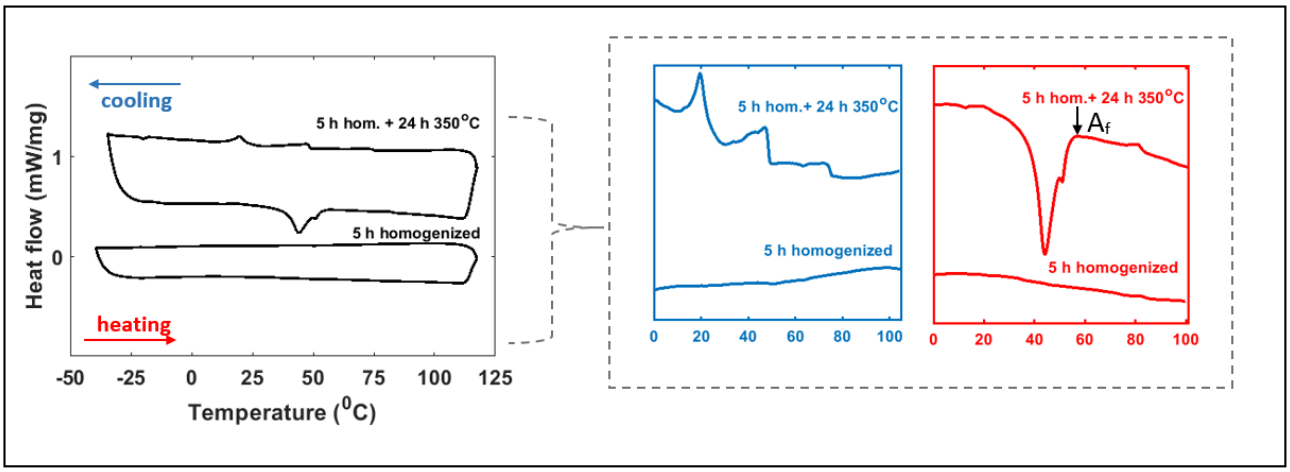

Figure 6: DSC plots of the samples subjected to 5 h of homogenization and then 24 h of aging at 350°C (The fluctuation around 75°C on the upper DSC plot in blue was attributed to an experimental noise that has been observed a few times with the same DSC equipment.)

In some studies, longer homogenization or aging of NiTi alloys are performed [38–40]. It is known that more secondary phases may dissolve into the matrix by increasing the homogenization time [39]. After 5 h of homogenization, transformation peaks disappeared from the DSC plot as shown in Figure 6; the material did not undergo any phase transformation in the studied temperature range. Figure 6 also shows the DSC plot obtained from the sample that was aged for 24 h at 350°C after homogenization. The A_f temperature was found to be around 55°C which is significantly higher than the ones obtained from the samples subjected to short time homogenization and aging treatments. The evolution of the phases by increasing the aging time from 1 to 24 h is discussed in the following paragraphs according to XRD analyzes.

XRD results of the heat treated samples are presented in Figure 7. Figure 7a shows a sharp decrease in the main austenite peak by 1 h of direct aging when compared to the XRD spectrum of the as-sintered specimen. According to the DSC plots in Figure 3, the samples are expected to be mixture of different phases (austenite, martensite and R-phases) at around room temperature, with a low austenite fraction. The slight XRD peak which showed up near 42° might be due to both a small fraction of the austenite phase [41] or R-phase diffraction that occurs between 42-43° [42, 43]. On the other hand, there was not much difference in the XRD spectrum of the directly aged samples depending on the aging temperature.

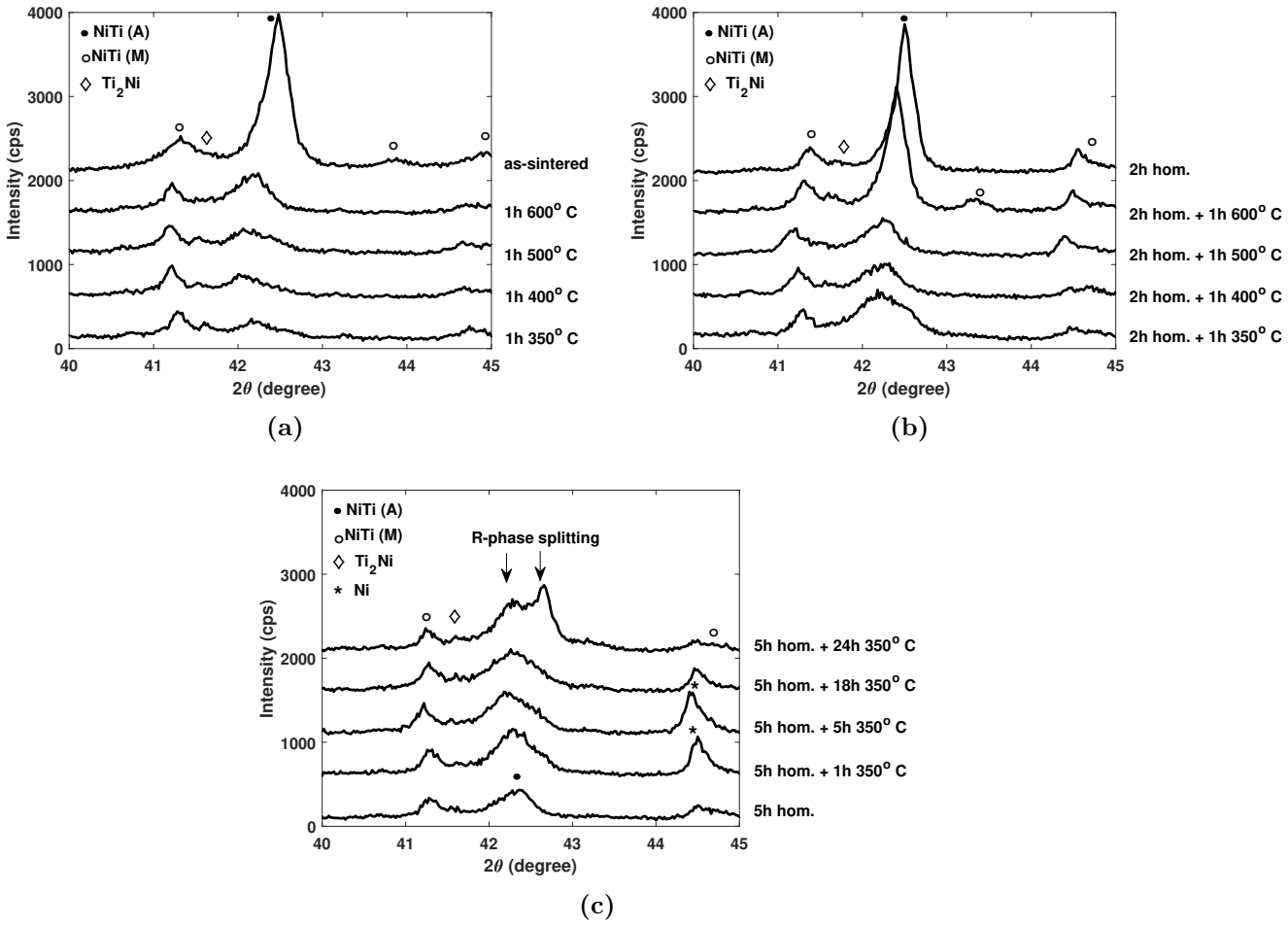

Figure 7: X-ray diffraction patterns of samples subjected to: a) 1 h of direct aging, b) 2 h of homogenization and 1 h of aging, c) 5 h of homogenization and aging at 350°C by varying time

Figure 7b shows XRD patterns obtained from the samples subjected to 2 h of homogenization plus 1 h of aging in the temperature range of $350 - 600$°C. XRD spectrum of the sample that was only homogenized contains austenite and martensite main phases with a high austenite intensity. The sample that was first homogenized and then aged at 600°C yielded a similar XRD spectrum. It is

consistent with the results obtained from the DSC study; both samples were mainly in the austenite phase at room temperature. The samples that were subjected to aging between 350-500°C were expected to be a mixture of austenite and R-phases according to their DSC plots in Figure 4. The XRD analysis also detected martensite peaks. It was shown in the literature that XRD can detect smaller volume fraction of phases when compared to thermal analyzes [44]. In general, XRD spectrum of the samples that were homogenized and then aged by 1 h at $350-400-500$°C were close, there was no secondary phase detected other than Ti_2Ni.

Figure 7c shows evolution of the XRD spectrum by increasing heat treatment duration at 350°C constant aging temperature. The samples were subjected to 5 h of homogenization and then aging for 1, 5, 18 and 24 h. After 5 h of homogenization, there were austenite and martensite phase peaks in the XRD spectrum. There was an evident increase in the intensity at the peak locations of free Ni element after 1-5 h of aging. The increase of the intensity and a relative angular shift of the peak location around 44.6° was attributed to a possible Ni release into the matrix. By increasing the aging time to 18-24 h, the intensity decreased, and a peak splitting was observed between 42-43° indicating the R-phase formation, a possible outcome of Ti_3Ni_4 precipitation in Ni-rich NiTi alloys achieved by heat treatment [16, 42].

High yield strength is one of the criteria for the pseudoelastic behavior of NiTi alloys. Micro-indentation analyzes showed the effect of heat treatment on the strength of the SPSed NiTi. According to the literature, aging affects the hardness of NiTi alloys by two main reasons. First, Ti_3Ni_4 precipitation alters the transformation temperatures by changing the Ni concentration of the matrix. As the difference between martensite start temperature and the test temperature increases, the resistance to martensitic transformation is enhanced, hence the increase of hardness. On the other hand, hardness is maximum at a small precipitate size. Therefore, assessment of hardness measurements must be done by considering both martensitic phase transformation and age hardening mechanisms [17,19,45].

In Figure 8, hardness and energy recovery follow the same trend in every heat treatment category; higher hardness accompanies higher energy recovery ratio. In general, average Vickers hardness and energy recovery ratios were found to be in the range of $200-250$ HV and $\%25-35$ respectively except for one sample which was subjected to long-time homogenization and aging at 350°C; the details of which will be given in the following paragraphs. Hardness of the as-sintered sample (~ 250 HV) was in the same order with NiTi alloys that were loaded to the same level in other studies. However, larger deviations were observed in hardness measurements of some specimens when compared to the ones provided in the literature [17, 32].

After 1 h of direct aging, there was no increase in the hardness compared to the as-sintered specimen as shown in Figure 8a. It was at a maximum at 400°C aging temperature, as well as the percent of recovered energy (Figure 8b). However, it is difficult to explain the differences in the hardness measurements of the samples in this group; first, it is unclear which phase was dominant during indentation of the samples by looking at their DSC plots, and their XRD spectrum were very close. Figures 8c and 8d show that hardness and energy recovery ratio decreased considerably by 2 h of homogenization. Usually, homogenization treatment results in softening of NiTi alloys due to dissolution of secondary phases such as Ti_2Ni [39] as it was the case in this study. Further aging for an hour, in $350-600$°C temperature range, did not result in a significant change in terms of hardness and energy recovery ratio. A relatively higher energy recovery was achieved by aging at 600°C as shown in Figure 8d. According to the DSC plots in Figure 4 and the XRD spectrum in Figure 7b, the samples which were subjected to 2 h of homogenization, and 2 h of homogenization plus 1 h of aging at 600°C were mainly in the austenite phase at the beginning of the indentation test, therefore, higher deformation recovery was attributed to the reversible martensitic transformation instead of precipitation hardening.

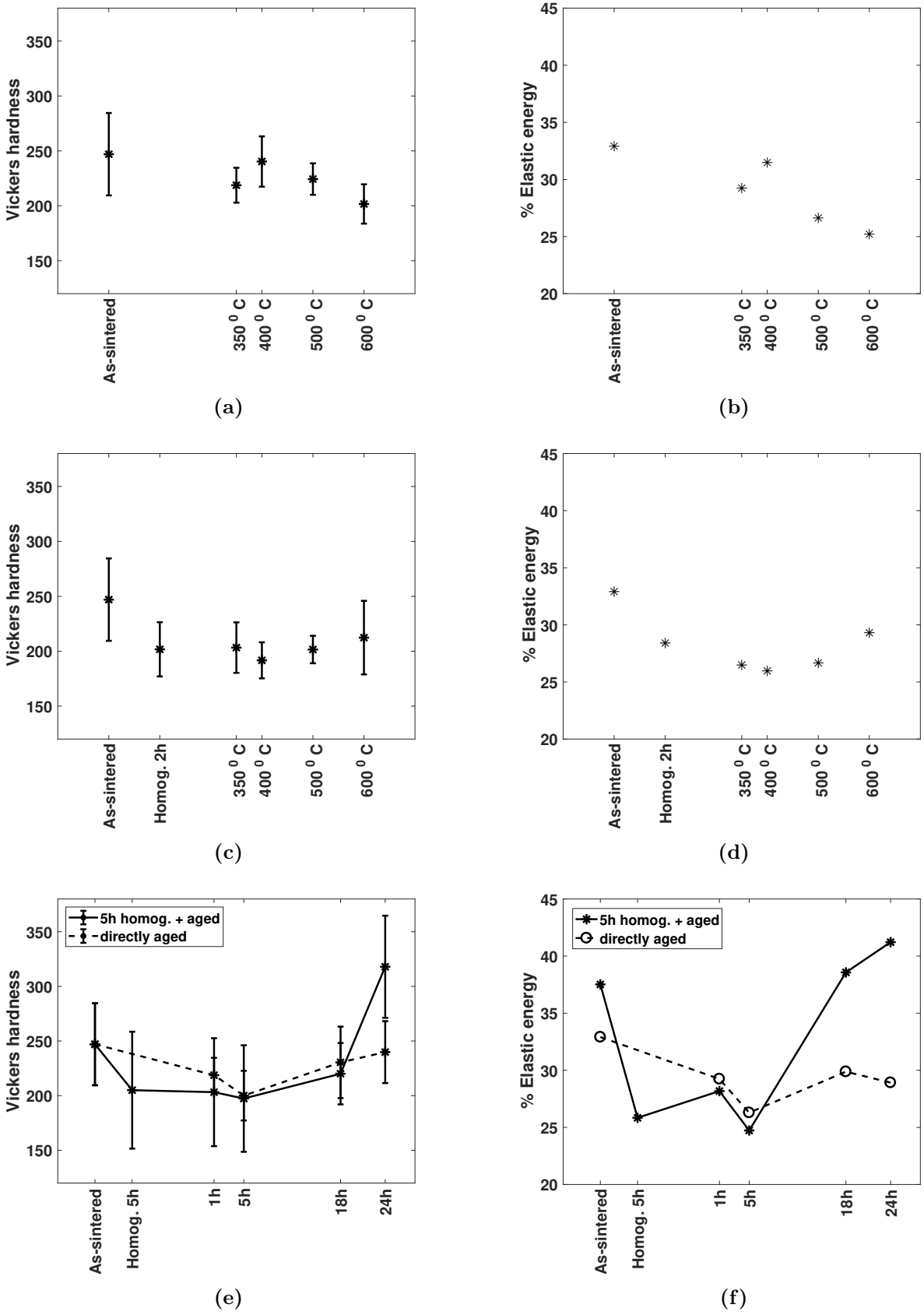

Figure 8: Vickers hardness and percentage of recoverable energy according to different heat treatments: a-b) 1 h direct aging at different temperatures, c-d) 2 h homogenization at 1000°C and then 1 h aging at different temperatures, e-f) aging at 350°C for different duration. Error bars represent the standard deviations in 10 measurements.

Strength of the alloy did not increase by the first two groups of heat treatments. In the third group of indentation analyzes, the material was subjected to aging treatment at 350°C for various hours. The samples were either first homogenized for 5 h and then aged or directly aged from 1 to 24 h. The most significant enhancement in the hardness and the energy recovery ratio was achieved by increasing the aging time to 24 h as shown in Figures 8e and 8f; the material that was first homogenized for 5 h and then aged for 24 h exhibited around 325 Vickers hardness, and %40 of energy recovery ratio. It is important that hardness and energy recovery ratio did not increase in the same way without homogenization prior to aging treatment; the hardness achieved by 24 h of direct aging treatment was in the same level with the as-sintered one.

Figure 9 shows the uniaxial stress-strain diagrams of the cylindrical compacts that were subjected to different thermal treatment. In general, some residual strain was observed indicating a deformation at the end of a partial-pseudoelastic loop which was not fully plastic. A significant portion of the residual strain was removed by re-heating the samples above A_f, and then cooling to room temperature as shown by the arrows on the stress-strain diagrams. It should be noted that the phase transformation continued gradually in a large temperature interval in the specimen which was subjected to 1 h of direct aging at 350°C (see Figure 3). Therefore, that sample was loaded at 45°C which is 5°C above the temperature that corresponds to the end of the main transformation peak observed during heating. At that temperature, the alloy was expected to be in austenite-martensite mixed structure. Therefore, the minimum strain recovery was achieved from the uniaxial compression of this specimen among all specimens that were tested in this study. The specimen that was subjected to 2 h of homogenization and then 1 h of aging at 350°C was expected to be in complete austenite phase at 45°C according to its DSC plot. The strain recovery achieved from this specimen was higher than the one that was directly aged at the same temperature as shown in Figure 9c. The maximum pseudoelastic strain recovery was achieved from the specimen that was subjected to 5 h of homogenization and then 24 h of aging at 350°C; around 50% of the deformation was recovered globally as shown in Figure 9e.

The stress-strain diagrams show that the material did not fully recover from the deformation after compression above A_f; some of the deformation was recovered back by reheating the samples until around 100°C and then cooling back to room temperature. The residual strain might be due to some amount of blocked martensite plates in addition to a small plastic deformation. In the literature, the full pseudoelastic behavior was observed by only a few researchers for alloys with either higher Ni concentration [20, 21] or produced with finer powders [22, 23]. A similar result was reported by McNeese et al. [31] for the uniaxial compression of NiTi samples processed by hot isostatic pressing. They also observed significant residual strain after uniaxial compression of the samples tested above their A_f temperature. The behavior was named as partial pseudoelastic, and it was attributed to the Ni concentration of the matrix (49 at.% Ni). The EDX analysis of the samples in this study also revealed around 49 at.% Ni concentration as presented in the previous discussion. On the other hand, the material underwent martensitic reorientation at room temperature as shown in Figure 9. At room temperature, the specimens were expected to be mostly in the martensite or R-phase, and the expected deformation mechanism was the martensitic reorientation. At the end of unloading, there was around 3% of residual strain which was almost completely recovered by reheating the specimens until around 100°C and then cooling back to room temperature. Although the pseudoelastic behavior was partial, the specimens from each category of heat treatment showed almost complete shape memory effect.

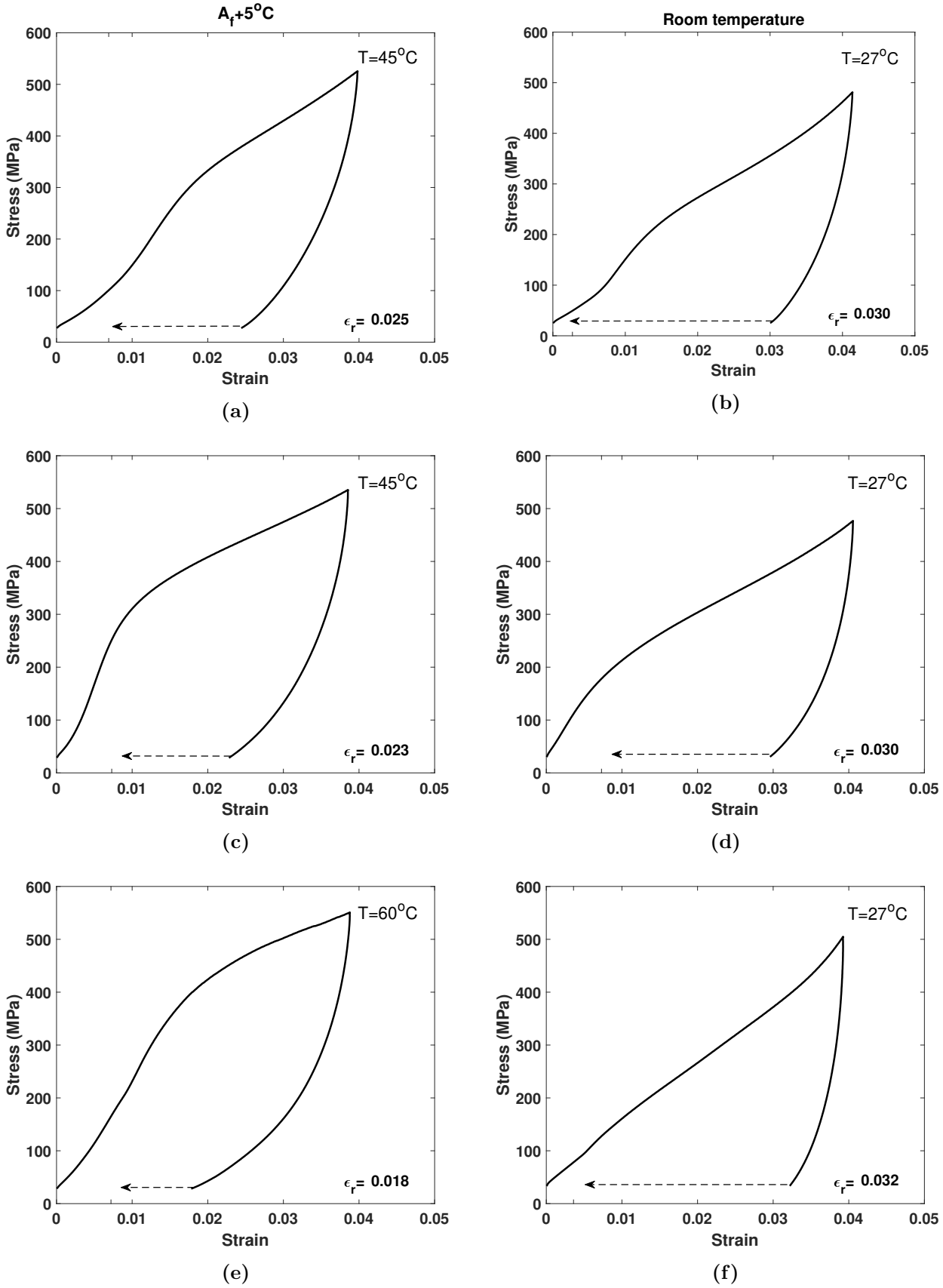

Figure 9: Stress-strain diagrams obtained from uniaxial compression of the samples subjected to: a-b) 1 h of direct aging at 350°C, c-d) 2 h of homogenization and then 1 h of aging at 350°C, e-f) 5 h of homogenization and then 24 h of aging at 350°C. Test temperatures are indicated at upper right corners. Figures on the left correspond to the tests 5°C above A_f temperature, Figures on the right correspond to the tests at room temperature (27°C). The residual strain at the end of unloading is presented inside each figure. Arrows represent the strain recovery by re-heating the samples until 100°C and then cooling to room temperature.

In general, it was shown that the transformation characteristics of the SPSed NiTi were similar to those of bulk NiTi alloys studied in the literature; aging favored the R-phase transformation under certain temperature and duration which affected the pseudoelastic behavior under uniaxial loading. When the specimens were compared in three categories, the pseudoelastic strain recovery achieved by direct aging or short time homogenization and aging treatments were lower. The maximum strain recovery was achieved from the specimen that was subjected to 5 h of homogenization plus 24 h of aging at 350°C. Micro-indentation results showed that this long aging treatment yielded the maximum hardness and energy recovery ratio, and it was the only case where the hardness increased considerably. DSC results in Figure 6 show that the sample was in R-phase at the temperature when indentation was performed, therefore, the high energy recovery obtained from the micro-indentation test cannot be solely related to reversible austenite to martensite transformation, a certain amount of coherent Ti_3Ni_4 precipitation must be present to enhance the resistance of the material against plastic deformation increasing the hardness and energy recovery. It is important that the long time aging treatment without prior homogenization did not result in the same age hardening mechanism showing that it is important to increase the homogeneity of the SPSed samples before aging.

4 Conclusions

This study was carried out on SPSed NiTi samples that have not shown the expected full pseudoelastic behavior under uniaxial compression. The samples were subjected to various heat treatments at different temperatures and duration, and were further analyzed using differential scanning calorimetry, X-ray diffraction, instrumented micro-indentation and uniaxial compression tests to discuss the effect of heat treatment on the phase transformation and the mechanical behavior. The main findings are summarized below.

The SPSed NiTi responded to homogenization and aging similar to bulk NiTi. With heat treatment, changes in the transformation sequence among austenite, martensite and R-phases were observed in DSC and XRD. Although the material did not show a complete pseudoelastic strain recovery under uniaxial compression, its pseudoelastic behavior was improved as a result of heat treatment. Among different heat treatments, the strain recovery was the lowest following direct aging: significant heterogeneity was observed in the DSC results. The homogenized samples resulted in more distinct transformation peaks when compared to the directly aged ones, and a slight improvement on the pseudoelastic response was observed under uniaxial compression. In general, moderate pseudoelastic behavior of the specimens was attributed to the Ni concentration of the matrix and to a large powder size at the initial state.

The maximum pseudoelastic strain recovery was obtained from the specimen that was subjected to 5 h of homogenization plus 24 h of aging at 350°C: more than 50% of deformation was recovered as shown in Figure 9e. Micro-indentation results showed that aging this long resulted in a considerable increase in hardness and energy recovery ratio through R-phase formation which is an expected outcome of precipitation hardening in NiTi alloys. Aging without first homogenizing did not increase the hardness showing the effect of homogenization on the SPSed samples' pseudoelastic behavior.

Data availability

The raw/processed data required to reproduce these findings cannot be shared at this time as the data also forms part of an ongoing study. They are available from the authors upon a proper request.

Declaration of competing interest

The authors declare that they have no known competing financial interests or personal relationships that could have appeared to influence the work reported in this paper.

CRediT author statement

Gülcan Özerim: Methodology, Conceptualization, Validation, Investigation, Writing - Original Draft, Visualization. **Günay Anlaş:** Methodology, Conceptualization, Validation, Resources, Writing - Review & Editing, Supervision, Project administration, Funding acquisition. **Ziad Moumni:** Methodology, Conceptualization, Validation, Resources, Writing - Review & Editing, Supervision, Project administration, Funding acquisition.

Acknowledgements

This research was partly funded by Boğaziçi University Resarch Fund (BAP) through the BAP project (project no 17741). Also, the author G.Ö. gratefully acknowledges the financial support of CampusFrance (the French Agency for the promotion of higher education, international student services, and international mobility) and ENSTA Paris-Institut Polytechnique de Paris.

Appendix A.

Additional data on spark plasma sintering is provided below.

Table A.1: Sintering parameters, resulting dimension and porosity of cylindrical compacts

	High density compact	Low density compacts			
Powder mass (g)	5.50	5.00	4.55	4.13	6.45
Mold diameter (mm)	8	8	8	8	10
Punch pressure (MPa)	60	60	60	60	38
Target temperature (°C)	1000	850	700	560	560
Duration at target temperature (min)	5	5	5	5	5
Final Length (mm)	17	16	15.3	15.9	18
Average porosity (%)	< 1	3.58	8.23	19.84	29.23

References

[1] Mohammad H. Elahinia, Mahdi Hashemi, Majid Tabesh, and Sarit B. Bhaduri. Manufacturing and processing of NiTi implants: A review. *Progress in Materials Science*, 57(5):911–946, 2012.

[2] Bin Yuan, Min Zhu, and Chi Yuen Chung. Biomedical porous shape memory alloys for hard-tissue replacement materials. *Materials*, 11(9), 2018.

[3] A. Bansiddhi, T. D. Sargeant, S. I. Stupp, and D. C. Dunand. Porous NiTi for bone implants: A review. *Acta Biomaterialia*, 4(4):773–782, 2008.

[4] X Wang, Y Li, Peter Hodgson, and Cuie Wen. Nano-and macro-scale characterisation of the mechanical properties of bovine bone. In *Materials forum*, volume 31, pages 156–159. Institute of Materials Engineering Australasia, 2007.

[5] M. Bram, A. Ahmad-Khanlou, A. Heckmann, B. Fuchs, H. P. Buchkremer, and D. Stöver. Powder metallurgical fabrication processes for NiTi shape memory alloy parts. *Materials Science and Engineering A*, 337(1-2):254–263, 2002.

[6] Y. Torres, J. J. Pavón, I. Nieto, and J. A. Rodríguez. Conventional powder metallurgy process and characterization of porous titanium for biomedical applications. *Metallurgical and Materials Transactions B: Process Metallurgy and Materials Processing Science*, 42(4):891–900, 2011.

[7] C. Velmurugan, V. Senthilkumar, Krishanu Biswas, and Surekha Yadav. Densification and microstructural evolution of spark plasma sintered NiTi shape memory alloy. *Advanced Powder Technology*, 29(10):2456–2462, 2018.

[8] ZA Munir, U Anselmi-Tamburini, and M Ohyanagi. The effect of electric field and pressure on the synthesis and consolidation of materials: A review of the spark plasma sintering method. *Journal of materials science*, 41(3):763–777, 2006.

[9] L. L. Ye, Z. G. Liu, K. Raviprasad, M. X. Quan, M. Umemoto, and Z. Q. Hu. Consolidation of MA amorphous NiTi powders by spark plasma sintering. *Materials Science and Engineering A*, 241(1-2):290–293, 1998.

[10] Bolu Liu, Shuigen Huang, Liugang Chen, Jan Van Humbeeck, and Jef Vleugels. Rapid synthesis of dense NiTi alloy through spark plasma sintering of a TiH2/Ni powder mixture. *Materials Letters*, 191:89–92, 2017.

[11] C. Shearwood, Y. Q. Fu, L. Yu, and K. A. Khor. Spark plasma sintering of TiNi nano-powder. *Scripta Materialia*, 52(6):455–460, 2005.

[12] Pavel Salvetr, Tomáš František Kubatík, Damien Pignol, and Pavel Novák. Fabrication of Ni-Ti Alloy by Self-Propagating High-Temperature Synthesis and Spark Plasma Sintering Technique. *Metallurgical and Materials Transactions B: Process Metallurgy and Materials Processing Science*, 48(2):772–778, 2017.

[13] Yinong Liu and S. P. Galvin. Criteria for pseudoelasticity in near-equiatomic NiTi shape memory alloys. *Acta Materialia*, 45(11):4431–4439, 1997.

[14] B. Yuan, X. P. Zhang, C. Y. Chung, and M. Zhu. The effect of porosity on phase transformation behavior of porous Ti-50.8 at.% Ni shape memory alloys prepared by capsule-free hot isostatic pressing. *Materials Science and Engineering A*, 438-440(SPEC. ISS.):585–588, 2006.

[15] K. Otsuka and X. Ren. Physical metallurgy of Ti-Ni-based shape memory alloys. *Progress in Materials Science*, 50(5):511–678, 2005.

[16] Jafar Khalil-Allafi, Antonin Dlouhy, and Gunther Eggeler. Ni4Ti3-precipitation during aging of NiTi shape memory alloys and its influence on martensitic phase transformations. *Acta Materialia*, 50(17):4255–4274, 2002.

[17] K. Gall, K. Juntunen, H. J. Maier, H. Sehitoglu, and Y. I. Chumlyakov. Instrumented micro-indentation of NiTi shape-memory alloys. *Acta Materialia*, 49(16):3205–3217, 2001.

[18] Antonin Dlouhy, Jafar Khalil-Allafi, and Gunther Eggeler. Multiple-step martensitic transformations in ni-rich niti alloys–an in-situ transmission electron microscopy investigation. *Philosophical Magazine*, 83(3):339–363, 2003.

[19] Carl P. Frick, Alicia M. Ortega, Jeffrey Tyber, A. El M. Maksound, Hans J. Maier, Yinong Liu, and Ken Gall. Thermal processing of polycrystalline NiTi shape memory alloys. *Materials Science and Engineering A*, 405(1-2):34–49, 2005.

[20] Ying Zhao, Minoru Taya, Yansheng Kang, and Akira Kawasaki. Compression behavior of porous NiTi shape memory alloy. *Acta Materialia*, 53(2):337–343, 2005.

[21] Sia Nemat-Nasser, Yu Su, Wei Guo Guo, and Jon Isaacs. Experimental characterization and micromechanical modeling of superelastic response of a porous NiTi shape-memory alloy. *Journal of the Mechanics and Physics of Solids*, 53(10):2320–2346, 2005.

[22] J Butler, P Tiernan, AA Gandhi, K McNamara, and SAM Tofail. Production of nitinol wire from elemental nickel and titanium powders through spark plasma sintering and extrusion. *Journal of materials engineering and performance*, 20(4-5):757–761, 2011.

[23] Ryoichi Soba, Yukiko Tanabe, Takayuki Yonezawa, Junko Umeda, and Katsuyoshi Kondoh. Microstructures and mechanical properties of shape memory alloy using pre-mixed TiNi powders with TiO2 particles. *Funtai Oyobi Fummatsu Yakin/Journal of the Japan Society of Powder and Powder Metallurgy*, 64(11):589–594, 2017.

[24] Pavel Salvetr, Jaromír Dlouhỳ, Andrea Školáková, Filip Prša, Pavel Novák, Miroslav Karlík, and Petr Haušild. Influence of heat treatment on microstructure and properties of niti46 alloy consolidated by spark plasma sintering. *Materials*, 12(24):4075, 2019.

[25] L. Zhang, Z. Y. He, Y. Q. Zhang, Y. H. Jiang, and R. Zhou. Enhanced in vitro bioactivity of porous NiTi-HA composites with interconnected pore characteristics prepared by spark plasma sintering. *Materials and Design*, 101:170–180, 2016.

[26] Ying Zhao and Minoru Taya. Processing of porous NiTi by spark plasma sintering method. *Smart Structures and Materials 2006: Active Materials: Behavior and Mechanics*, 6170(April 2006):617013, 2006.

[27] L. Zhang, Y. Q. Zhang, Y. H. Jiang, and R. Zhou. Superelastic behaviors of biomedical porous NiTi alloy with high porosity and large pore size prepared by spark plasma sintering. *Journal of Alloys and Compounds*, 644:513–522, 2015.

[28] L. Zhang, Z. Y. He, J. Tan, Y. Q. Zhang, M. Stoica, K. G. Prashanth, M. J. Cordill, Y. H. Jiang, R. Zhou, and J. Eckert. Rapid fabrication of function-structure-integrated NiTi alloys: Towards a combination of excellent superelasticity and favorable bioactivity. *Intermetallics*, 82:1–13, 2017.

[29] Zhiqiang Guo, Huimin Xie, Fulong Dai, Haichang Qiang, Lijian Rong, Pengwan Chen, and Fenglei Huang. Compressive behavior of 64% porosity NiTi alloy: An experimental study. *Materials Science and Engineering A*, 515(1-2):117–130, 2009.

[30] Martin Bram, Manuel Köhl, Hans Peter Buchkremer, and Detlev Stöver. Mechanical properties of highly porous NiTi alloys. *Journal of Materials Engineering and Performance*, 20(4-5):522–528, 2011.

[31] Matthew D. McNeese, Dimitris C. Lagoudas, and Thomas C. Pollock. Processing of TiNi from elemental powders by hot isostatic pressing. *Materials Science and Engineering A*, 280(2):334–348, 2000.

[32] Soheil Saedi, Ali Sadi Turabi, Mohsen Taheri Andani, Christoph Haberland, Haluk Karaca, and Mohammad Elahinia. The influence of heat treatment on the thermomechanical response of Ni-rich NiTi alloys manufactured by selective laser melting. *Journal of Alloys and Compounds*, 677:204–210, 2016.

[33] Eugene A Olevsky, William L Bradbury, Christopher D Haines, Darold G Martin, and Deepak Kapoor. Fundamental aspects of spark plasma sintering: I. experimental analysis of scalability. *Journal of the American Ceramic Society*, 95(8):2406–2413, 2012.

[34] ASTM F2004-17. Standard test method for transformation temperature of nickel-titanium alloys by thermal analysis. *ASTM International, West Conshohocken, PA*, 2017.

[35] Ruonan Qin, Fengchun Jiang, Mengxin Cao, Yanchun Li, Hexin Zhang, Chunhuan Guo, and Zhenqiang Wang. Preparation, microstructure and compressive property of niti alloy hollow spheres fabricated by powder metallurgy. *Materials Today Communications*, 30:103039, 2022.

[36] Juliane Mentz, Jan Frenzel, Martin F.X. Wagner, Klaus Neuking, Gunther Eggeler, Hans Peter Buchkremer, and Detlev Stöver. Powder metallurgical processing of NiTi shape memory alloys with elevated transformation temperatures. *Materials Science and Engineering A*, 491(1-2):270–278, 2008.

[37] M. R. Aboutalebi, M. Karimzadeh, M. T. Salehi, S. M. Abbasi, and M. Morakabati. Influences of aging and thermomechanical treatments on the martensitic transformation and superelasticity of highly Ni-rich Ti-51.5 at.% Ni shape memory alloy. *Thermochimica Acta*, 616:14–19, 2015.

[38] Soheil Saedi, Ali Sadi Turabi, Mohsen Taheri Andani, Narges Shayesteh Moghaddam, Mohammad Elahinia, and Haluk Ersin Karaca. Texture, aging, and superelasticity of selective laser melting fabricated Ni-rich NiTi alloys. *Materials Science and Engineering A*, 686(January):1–10, 2017.

[39] A Foroozmehr, A Kermanpur, F Ashrafizadeh, and Y Kabiri. Investigating microstructural evolution during homogenization of the equiatomic niti shape memory alloy produced by vacuum arc remelting. *Materials Science and Engineering: A*, 528(27):7952–7955, 2011.

[40] Cheng Lin Chu, Jonathan Cy Chung, and Paul K. Chu. Effects of heat treatment on characteristics of porous Ni-rich NiTi SMA prepared by SHS technique. *Transactions of Nonferrous Metals Society of China (English Edition)*, 16(1):49–53, 2006.

[41] Manjunatha Pattabi, K Ramakrishna, and KK Mahesh. Effect of thermal cycling on the shape memory transformation behavior of niti alloy: powder x-ray diffraction study. *Materials Science and Engineering: A*, 448(1-2):33–38, 2007.

[42] JI Kim, Yinong Liu, and S Miyazaki. Ageing-induced two-stage r-phase transformation in ti–50.9 at.% ni. *Acta Materialia*, 52(2):487–499, 2004.

[43] Jéssica Dornelas Silva, Suzanny Cristina Martins, Natalia Isabel de Azevedo Lopes, Pedro Damas Resende, Leandro Arruda Santos, and Vicente Tadeu Lopes Buono. Effects of aging treatments on the fatigue resistance of superelastic niti wires. *Materials Science and Engineering: A*, 756:54–60, 2019.

[44] J Uchil, FM Braz Fernandes, and KK Mahesh. X-ray diffraction study of the phase transformations in niti shape memory alloy. *Materials characterization*, 58(3):243–248, 2007.

[45] R Liu, DY Li, YS Xie, R Llewellyn, and HM Hawthorne. Indentation behavior of pseudoelastic tini alloy. *Scripta Materialia*, 41(7):691–696, 1999.

The effect of heat treatment on pseudoelastic behavior of spark plasma sintered NiTi

1 **Fabrication** → 2 **Heat Treatment** → 3 **Calorimetric Tests** → 4 **Microstructure Evaluation**

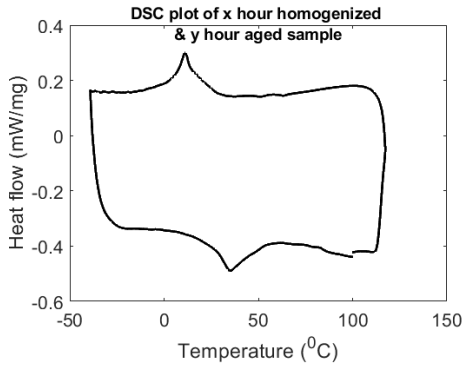

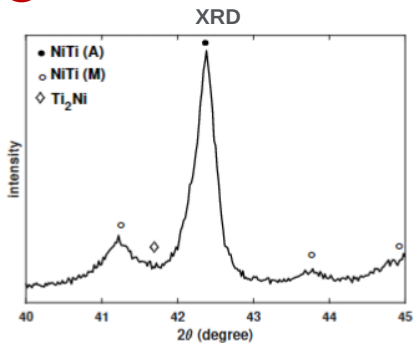

6 **Uniaxial Compression (High temp. & room temp.)** ← 5 **Micro-indentation: Hardness & Energy Recovery**